Incompressibility and symmetry energy of a neutron star

Ankit Kumar,* H. C. Das,† and S. K. Patra‡
Institute of Physics, Sachivalaya Marg, Bhubaneswar 751005, India
and Homi Bhabha National Institute, Training School Complex, Anushakti Nagar, Mumbai 400094, India

(Received 10 May 2021; revised 7 September 2021; accepted 5 November 2021; published 22 November 2021)

We trace a systematic and consistent method to precisely numerate the magnitude range for various structural and isospin compositional properties of the neutron star. Incompressibility, symmetry energy, slope parameter, and curvature of a neutron star are investigated using the relativistic energy density functional within the framework of coherent density fluctuation model. The analytical expression for the energy density functional of the neutron star matter is motivated from the Brückner functional and acquired by the polynomial fitting of the saturation curves for three different relativistic mean-field parameter sets (NL3, G3, and IU-FSU). The modified functional is folded with the neutron star's density-dependent weight function to calculate the numerical values for incompressibility and symmetry energy using the coherent density fluctuation model. The NL3 parameter set, being the stiffest equation of state, has a higher magnitude of all the properties compared to the other two parameter sets.

DOI: 10.1103/PhysRevC.104.055804

Neutron stars, being surprisingly dense objects in the universe, are impressive to both astrophysicists and nuclear physicists. Astronuclear physicists perceive the neutron star as having an enormously large nucleus bound by the gravity and are amazed by its short-range strong nuclear interactions and enormous gravitational and electromagnetic interactions. An understanding of the properties of neutron stars demands thorough knowledge of both astrophysics and nuclear physics, which are mostly incoherent. A conformability exits between the astral properties (i.e., gravitational potential, central temperature, angular velocity, magnetic poles) and the nuclear properties (i.e., baryon density, neutrino emissivity, isospin asymmetry, superconductivity) of neutron stars [1]. However, there are some properties of the neutron stars like pressure, incompressibility, and symmetry energy which are significant for experimental and theoretical explanations of its nontrivial behavior.

The consequences of "symmetry" are essential to many important aspects of the modern physics. Theoretical modeling of the analytical and structural behavior of highly asymmetric dense nuclear matter (NM) depends significantly on the symmetry energy [2]. Also, the parameters derived by expanding the symmetry energy around saturation density (slope and curvature parameter) control the core-crust transition density, transition pressure, and the cooling rate of the neutron stars [3,4]. The quantitative information on the slope and curvature parameter of the neutron stars can be applied to constrain the equation of state (EoS) obtained using different parameter sets of the vast relativistic framework. The particle fraction in the core of the neutron stars, which is a critical quantity to the cooling of neutron stars, is also controlled by the domain of symmetry energy and slope parameter [5]. Since symmetry energy cannot be measured directly, the elucidation of experimentally available data requires a substantial and consistent theoretical model for nuclear matter at very high densities [6–8]. The precise range of the symmetry energy for the isospin asymmetric nuclear matter and the neutron stars has been a debatable issue among researchers. Along with the theoretical calculations, laboratory nuclear experiments (i.e., giant dipole resonance, heavy-ion collisions, neutron skin) and abridged results of astrophysical observations (i.e., mass-radius profile, dimensional tidal deformability) have also constrained the domain of symmetry energy and its derivatives [9–12]. Another important quantity which controls the equation of state (EoS) of any dense matter system is incompressibility.

Dependence of incompressibility on the isospin asymmetry parameter of the nuclear system restricts the stiffness of the EoS, which indirectly influences the maximum mass and radius of the neutron star, e.g., maximally compressible dense matter handles the upper limit on the maximum mass of the neutron star [13]. The quantitative dimension of the incompressibility coefficient also helps in the determination of angular velocity and the evolution of cooling stage of the rapidly rotating neutron stars [14]. The collective motion of the nucleons inside a nucleus produces nuclear giant resonances, which are a global feature of the finite nuclei [15,16]. The isoscalar giant monopole resonance (ISGMR) is the most common collective oscillation with both protons and neutrons in same phase. This ISGMR is the breathing mode oscillation related to the incompressibility K_A of the finite nucleus of mass A. Thus, the nuclear incompressibility K_A is a vital quantity for understanding the various modes of oscillations of the finite

*ankit.k@iopb.res.in
†harish.d@iopb.res.in
‡patra@iopb.res.in

nucleus [17,18]. Similarly, the other modes of collective oscillations, such as isovector giant dipole resonance (IVGDR) and isoscalar [isovector] giant quadrupole resonances (ISGQR [IVGQR]) are also governed by nuclear incompressibility and the other symmetry-related parameters of the finite nucleus. The various collective resonances decide the internal structures of the finite nucleus; for example, the IVGDR tells the shape of the nucleus and the ISGMR gives information about the compression or expansion capacity of the nucleus. The calculations of the monopole and quadrupole excitation energies and their relations with incompressibility using various sum rule approaches are demonstrated in Refs. [19,20]. For a particular model, either a relativistic or a nonrelativistic, to be consistent with the constraints set by the terrestrial or astrophysical experiments, the nuclear incompressibility, symmetry energy, and other related quantities are essential. Neutron stars (NS), which have huge nuclei with mass number $A \approx 10^{57}$, must possess all the natural properties of practical finite nuclei, such as all types of collective oscillations. The incompressibility $K^{\rm star}$, symmetry energy $S^{\rm star}$, and higher derivatives such as $L^{\rm star}_{\rm sym}$ and $K^{\rm star}_{\rm sym}$ are informative and necessary to explore the structure of the neutron star. In the present paper, our aim is to discuss another approach, coherent density fluctuation model (CDFM), for the evaluation of these quantities of neutron stars. This model is applicable for a neutron star, as it has a finite surface like that of a standard nucleus. Here, we provide an approach to calculate both of these parameters (symmetry energy and incompressibility) for a neutron star matter system in a consistent and accurate manner.

In the past few decades, the theoretical models destined to explore the behavior of a dense nuclear medium have been useful to unravel the properties of compact astrophysical objects, i.e., neutron stars or white dwarfs. The structural and compositional resemblance of finite nuclei and neutron stars indicate that the physics of compact objects can be explored by extrapolating the data of terrestrial experiments and theoretical formulation of dense matter systems [21]. From the states of highly dense matter in the inner core to the pasta phases of nuclei at ordinary densities in the outer crust, a neutron star manifests the thorough distribution of matter [22]. Neutron star cores are 10^3 times or more dense than at "neutron drip" line, so, we can utilize a consistent, congruous, and ultrahigh-density equation of state of nuclear matter for an understanding of neutron star properties [23]. Comprehensive knowledge of the EoS of nuclear matter and pure neutron matter indicates a bridge between the finite nuclei and dense interstellar bodies. The EoS of strongly interacting dense matter is the key component for the determination of general properties of neutron star (maximum mass, radius, tidal deformability) and it also controls the cooling rate and dynamics of core-collapse supernovae remnants [4,24]. Immobilizing the correct EoS for the compact stellar objects had been a complex task in nuclear and astroparticle physics over the past few decades. Several constraints had been enforced on the EoS at high density with the help of observational gravitational wave data (GW170817) [25], the Einstein Observatory (HEAO-2) [26], and various generations of x-ray radio telescopes [27,28]. There are many nonrelativistic (Skyrme [29], Gogny forces [30]) and relativistic (relativistic mean-field model [31,32]) theoretical approaches which provide a consistent formalism to construct the EoS and calculate the empirical properties of strongly interacting dense matter systems, which we can adopt as a manifestation of compact stars. The relativistic class of models are an alternative and more factual approach for low-energy quantum chromodynamics with all the built-in nonperturbative properties (i.e., current conservation, local or global symmetry breaking, etc.), where baryons and nuclei are stabilized as solitons in a mesonic fluid [33,34]. With the advancement in the cumbersome algebra of quantum field theory, the effective interaction between the nucleons and mesons can be expressed in the form of energy density functionals., which can be approached with the help of self-consistent relativistic mean-field (RMF) model.

In this work, we apply the RMF formalism to obtain the EoS for a dense matter system, where along with the neutrons and protons, electrons are also present to maintain the charge neutrality. We denote this kind of infinite dense matter (consisting of neutron, proton, and electron) as neutron star matter (NSM). Since our aim here is to calculate the properties for a neutron star, it is necessary to add electrons and muons in our system to maintain the compositional and neutrality properties of the star. Now, the Lagrangian for such a dense matter within RMF formalism can be written as [9]

$$
\begin{aligned}
\mathcal{L} = \sum_{i=p,n} \bar{\psi}_i \Bigg\{ \gamma_\nu \Bigg(i\partial^\nu - g_\omega \omega^\nu - \frac{1}{2} g_\rho \vec{\tau}_i \cdot \vec{\rho}^{\,\nu} \Bigg) - (M - g_\sigma \sigma \\
- g_\delta \vec{\tau}_i \cdot \vec{\delta}) \Bigg\} \psi_i + \frac{1}{2} \partial^\nu \sigma \, \partial_\nu \sigma - \frac{1}{2} m_\sigma^2 \sigma^2 + \frac{\zeta_0}{4!} g_\omega^2 (\omega^\nu \omega_\nu)^2 \\
- g_\sigma \frac{m_\sigma^2}{M} \left(\frac{\kappa_3}{3!} + \frac{\kappa_4}{4!} \frac{g_\sigma}{M} \sigma \right) \sigma^3 + \frac{1}{2} m_\omega^2 \omega^\nu \omega_\nu - \frac{1}{4} F^{\nu\alpha} F_{\nu\alpha} \\
+ \frac{1}{2} \frac{g_\sigma \sigma}{M} \left(\eta_1 + \frac{\eta_2}{2} \frac{g_\sigma \sigma}{M} \right) m_\omega^2 \omega^\nu \omega_\nu + \frac{1}{2} \eta_\rho \frac{m_\rho^2}{M} g_\sigma \sigma (\vec{\rho}^{\,\nu} \cdot \vec{\rho}_\nu) \\
+ \frac{1}{2} m_\rho^2 \rho^\nu \cdot \rho_\nu - \frac{1}{4} \vec{R}^{\nu\alpha} \cdot \vec{R}_{\nu\alpha} - \Lambda_\omega g_\omega^2 g_\rho^2 (\omega^\nu \omega_\nu)(\vec{\rho}^{\,\nu} \cdot \vec{\rho}_\nu) \\
+ \frac{1}{2} \partial^\nu \vec{\delta} \, \partial_\nu \vec{\delta} - \frac{1}{2} m_\delta^2 \vec{\delta}^{\,2} + \sum_{l=e,\mu} \bar{\phi}_l \, (i\gamma_\nu \partial^\nu - m_l) \phi_l, \qquad (1)
\end{aligned}
$$

where the last term stands for the added electrons and muons in the nuclear matter and ψ, $\bar{\psi}$, ϕ_l are the wave functions of the nucleons (proton and neutron), antinucleons, and leptons respectively. It includes σ, ω, ρ, and δ mesons to represent the interaction of nucleons, self- and cross-coupled interactions. M stands for the mass of the nucleons; m_σ, m_ω, m_ρ, m_δ, g_σ, g_ω, g_ρ, and g_δ are the masses and the self-coupling constants for σ, ω, ρ, and δ mesons respectively; κ_3, κ_4, ζ_0, η_1, η_2, η_ρ, and Λ_ω are the coupling constants; $F^{\nu\alpha}$ and $\vec{R}^{\nu\alpha}$ are field strengths; and τ_3 is the isospin operator. A more detailed explanation of the Lagrangian is discussed in Refs. [9,35–37]. We obtain the EoS for the defined neutron star matter by applying the Euler-Lagrange's equation of motion and the relativistic mean-field approximation on the above Lagrangian [Eq. (1)] [35,38]. To get a comprehensive idea of the EoS, we derive the EoS

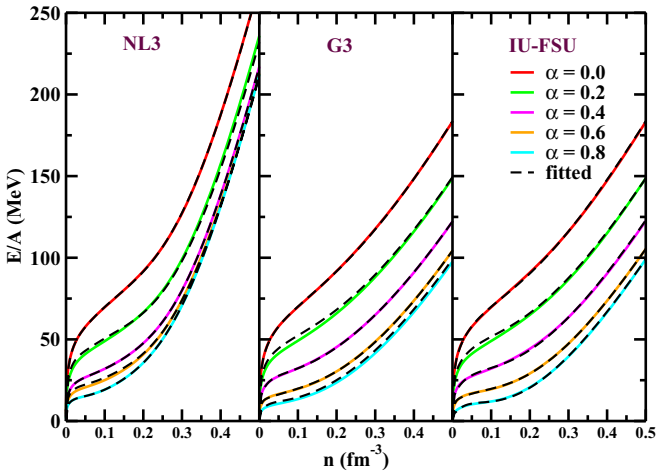

FIG. 1. The neutron star matter saturation curves as a function of baryon number density for different asymmetry $\alpha = \frac{n_n - n_p}{n_n + n_p}$ parameter. The solid curve represents the RMF numerical data and the dotted black curve stands for the fitted expression.

for the complete range of asymmetry factor. The asymmetry parameter (α) is defined as $\alpha = \frac{n_n - n_p}{n_n + n_p}$, with n_n and n_p being the neutron and proton densities, and $\alpha = 1$ stands for purely neutron matter. The number density of electrons and muons in the neutron star matter is kept equal to the proton number density to maintain the charge neutrality, i.e.,

$$n_p = n_e + n_\mu. \tag{2}$$

The binding energy per nucleon ($E/n - M$, where E is the energy density and n is the total nucleon density) curve as a function of nucleonic number density is depicted in Fig. 1.

In the present work, we used three different RMF parameter sets (NL3 [39], G3 [36], and IU-FSU [40]), with NL3 being the stiffest and the recently developed G3 being the softest, which compose the whole range of equation of state. The values of nuclear matter properties (i.e., saturation density, binding energy, incompressibility, etc.) for symmetric nuclear matter predicted by the chosen RMF parameter sets satisfy all the empirical and experimental constraints. The numerical magnitudes of incompressibility of symmetric nuclear matter (K) at saturation density for G3 and IU-FSU forces are 244 and 231 MeV, and those of symmetry energy (S) are 31 and 32 MeV, respectively [9,41], which are appropriate for the range stated by various theoretical and experimental models [42,43]. The three considered parameter sets are widely used in literature and our aim is to show the variation of the results with different forces. It is to be noted here that NL3 is one of the most successful parameter sets for finite nuclei. This set is also used to explain the GW190814 data with a mixture of dark matter inside the neutron star [44]. The coupling constants and the nuclear matter properties at saturation density along with the empirical and experimental values are presented in Table I.

To achieve an expressional form of energy functional for the effective interactions in the neutron star matter explained by RMF formalism, we have fitted the numerically obtained data. The assumptive form of the fitted energy functional is

TABLE I. The coupling constants and the nuclear matter properties at saturation for the EoS of NL3 [39], G3 [36], and IU-FSU [40] parameter sets. The nucleon mass (M) is 939.0 MeV. All of the coupling parameters are dimensionless and the NM parameters are in MeV, except n_0 which is in fm^{-3}. The NM parameters are given at saturation density for NL3, G3, and IU-FSU parameter sets in the lower panel.

Parameter	NL3	G3	IU-FSU	Empirical/Expt. value
m_σ/M	0.541	0.559	0.523	0.426–0.745[a]
m_ω/M	0.833	0.832	0.833	0.833–0.834[b]
m_ρ/M	0.812	0.820	0.812	0.825–0.826[c]
m_δ/M	0.0	1.043	0.0	1.022–1.064[d]
$g_\sigma/4\pi$	0.813	0.782	0.793	
$g_\omega/4\pi$	1.024	0.923	1.037	
$g_\rho/4\pi$	0.712	0.962	1.081	
$g_\delta/4\pi$	0.0	0.160	0.0	
k_3	1.465	2.606	1.1593	
k_4	−5.688	1.694	0.0966	
ζ_0	0.0	1.010	0.03	
η_1	0.0	0.424	0.0	
η_2	0.0	0.114	0.0	
η_ρ	0.0	0.645	0.0	
Λ_ω	0.0	0.038	0.046	
n_0	0.148	0.148	0.154	0.148–0.185[e]
$B.E.$	−16.29	−16.02	−16.39	−15.00–17.00[f]
K	271.38	243.96	231.31	220–260[g]
S	37.43	31.84	32.71	30.20–33.70[h]
$L_{\rm sym}$	120.65	49.31	49.26	35.00–70.00[i]
$K_{\rm sym}$	101.34	−106.07	23.28	−174–−31[j]
$Q_{\rm sym}$	177.90	915.47	536.46	

[a]Reference [45].
[b]Reference [45].
[c]Reference [45].
[d]Reference [45].
[e]Reference [46].
[f]Reference [46].
[g]Reference [42].
[h]Reference [43].
[i]Reference [43].
[j]Reference [47].

motivated by the work of Brückner *et al.* [48,49]. There are several issues with Brückner's energy functional; for instance, it cannot rectify the Coester-band problem [50] and it is defined purely for the nonrelativistic nuclear matter formalism. We ameliorate the Brückner energy functional in the local density approximation, so that it can satisfy the RMF data [51] and also added some series of potential function and an extra term for the lepton's kinetic energy inclusion. The modified energy density functional can be stated as

$$\mathcal{E} = C_k n^{2/3} + C_e n^{4/9} + \sum_{i=3}^{14} (b_i + a_i \alpha^2) n^{i/3}, \tag{3}$$

where $C_k = 0.3(\hbar^2/2M)(3\pi^2)^{2/3}[(1+\alpha)^{5/3} + (1-\alpha)^{5/3}]$ [49] is the kinetic energy coefficient for nucleons and $C_e = b_e(1-\alpha)^{5/9}$, with b_e as a variable obtained during fitting procedure, is the kinetic term coefficient for

leptons. The last term stands for the potential interaction of the nucleons and the coefficients b_i and a_i have to be obtained by fitting procedure for different RMF parameter sets. We observed that the accuracy of the fitting mechanism decreases if we reduce the number of coefficients (a_i and b_i) in the expansion of potential term of Eq. (3) [51]. The mean deviation δ, which is defined as $\delta = [\sum_{j=1}^{N}(E/A)_{j,\text{Fitted}} - (E/A)_{j,\text{RMF}}]/N$, with N being the total number of points, is 18%, 6%, and 0.5% for 8 [i.e., i runs from 3 to 10 in Eq. (3)], 10, and 12 terms respectively. The fitted curves of the neutron star matter with the above expression [Eq. (3)] are shown in the Fig. 1 through the black dotted lines. We have used this energy density functional as an input in the coherent density fluctuation method to achieve the range of certain properties of neutron star (incompressibility, symmetry energy, and slope parameter). Coherent density fluctuation model (CDFM) was first introduced three decades ago by Antonov *et al.* and is now a well-established formalism to decipher the properties of finite nuclei [52–54]. The backbone of the CDFM model is that a coordinate generator x can be used to write the one-body density matrix $n(r, r')$ of a nucleus as a sequential superposition of infinite number of one-body density matrices $n_x(r, r')$, which are termed "fluctons" [55,56]. The density of fluctons has the form

$$n_x(\mathbf{r}) = n_0(x)\,\Theta(x - |\mathbf{r}|), \tag{4}$$

where $n_0(x)$ is defined as $n_0(x) = 3A/4\pi x^3$, with A being the total number of nucleons in the finite matter. Within the CDFM approach, the density distribution of the spherical finite nuclear matter of radius r can be expressed as [57,58]

$$n(r) = \int_0^\infty dx\,|F(x)|^2\,n_0(x)\,\Theta(x - |\mathbf{r}|), \tag{5}$$

$|F(x)|^2$ is defined as the weight function and it can be obtained theoretically for a monotonically decreasing local density in the generator coordinate x as [57]

$$|F(x)|^2 = -\frac{1}{n_0(x)}\frac{dn(r)}{dr}\bigg|_{r=x}. \tag{6}$$

Now, the nuclear and structural properties of the neutron star, i.e., incompressibility (K^{star}), symmetry energy (S^{star}), slope parameter ($L_{\text{sym}}^{\text{star}}$), and curvature ($K_{\text{sym}}^{\text{star}}$), can be expressed in terms of weight function and the expression of the parameters evaluated from the energy density functional [Eq. (3)] of infinite star matter system as [55,58,59]

$$K^{\text{star}} = \int_0^\infty dx\,|F(x)|^2\,K^{\text{NSM}}(n(x)), \tag{7}$$

$$S^{\text{star}} = \int_0^\infty dx\,|F(x)|^2\,S^{\text{NSM}}(n(x)), \tag{8}$$

$$L_{\text{sym}}^{\text{star}} = \int_0^\infty dx\,|F(x)|^2\,L_{\text{sym}}^{\text{NSM}}(n(x)), \tag{9}$$

$$K_{\text{sym}}^{\text{star}} = \int_0^\infty dx\,|F(x)|^2\,K_{\text{sym}}^{\text{NSM}}(n(x)), \tag{10}$$

The profile of the weight function with density holds key information about the dependence of the calculated properties on the structure and composition of the defined matter system. The magnitude of the weight function at a value of x will decide the share of that particular region of density in the overall magnitude of calculated property. The energy density functional for the neutron star matter can be converted from momentum space to the coordinate space x in a local density approximation technique using the Brückner method. The expressions for K^{NSM}, S^{NSM}, $L_{\text{sym}}^{\text{NSM}}$, and $K_{\text{sym}}^{\text{NSM}}$ can be obtained from Eq. (3) by applying their common derivative definitions [60–62]; i.e., the NM parameters K^{NM}, S^{NM}, $L_{\text{sym}}^{\text{NM}}$, and $K_{\text{sym}}^{\text{NM}}$ are obtained from the following standard relations:

$$K^{\text{NM}} = 9\rho_0^2\frac{\partial^2}{\partial\rho^2}\left(\frac{\mathcal{E}}{\rho}\right)\bigg|_{\rho=\rho_0}, \tag{11}$$

$$S^{\text{NM}} = \frac{1}{2}\frac{\partial^2(\mathcal{E}/\rho)}{\partial\alpha^2}\bigg|_{\alpha=0}, \tag{12}$$

$$L_{\text{sym}}^{\text{NM}} = 3\rho_0\frac{\partial S(\rho)}{\partial\rho}\bigg|_{\rho=\rho_0} = \frac{3P}{\rho_0}, \tag{13}$$

$$K_{\text{sym}}^{\text{NM}} = 9\rho_0^2\frac{\partial^2 S(\rho)}{\partial\rho^2}\bigg|_{\rho=\rho_0}. \tag{14}$$

which are given as follows using Eq. (3):

$$K^{\text{NSM}} = -150.12\,n_0^{2/3}(x) - 2.22\,b_e\,n_0^{4/9}(x) + \sum_{i=4}^{14} i\,(i-3)\,b_i\,n_0^{i/3}(x), \tag{15}$$

$$S^{\text{NSM}} = 41.7\,n_0^{2/3}(x) - 0.12\,b_e\,n_0^{4/9}(x) + \sum_{i=3}^{14} a_i\,n_0^{i/3}(x), \tag{16}$$

$$L_{\text{sym}}^{\text{NSM}} = 83.4\,n_0^{2/3}(x) - 0.16\,b_e\,n_0^{4/9}(x) + \sum_{i=3}^{14} i\,a_i\,n_0^{i/3}(x), \tag{17}$$

$$K_{\text{sym}}^{\text{NSM}} = -83.4\,n_0^{2/3}(x) + 0.266\,b_e\,n_0^{4/9}(x) + \sum_{i=4}^{14} i\,(i-3)\,a_i\,n_0^{i/3}(x), \tag{18}$$

The above expressions are derived for the symmetric ($\alpha = 0$) case. Now, we can easily calculate the nuclear properties of the neutron star with the help of the weight function and using the above expressions. The weight function computation demand the slope of density curve with respect to the radius of the neutron star. We compute the mass-radius profile and the density curve of the neutron star for the three considered RMF parameter sets. The density curve and the mass-radius profile of the neutron star can be acquired by imposing the β equilibrium conditions [9,63] in the neutron star matter and using the obtained EoS as an input for the Tolman-Oppenheimer-Volkoff (TOV) equations [64,65]. The β- equilibrium conditions and the TOV equations for the static isotropic protoneutron star can be written as

$$\mu_n = \mu_p + \mu_e,$$
$$\mu_e = \mu_\mu, \tag{19}$$

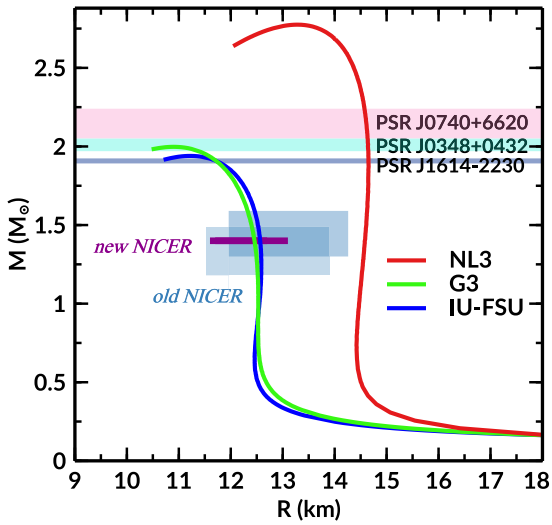

FIG. 2. Mass-radius profile of a neutron star for NL3 (red), G3 (green), and IU-FSU (blue) parameter sets. The old NICER data is given in two boxes from the two different analyses [67,68]. The horizontal line in violet color represents the new NICER constraint on the radius of the canonical star [69].

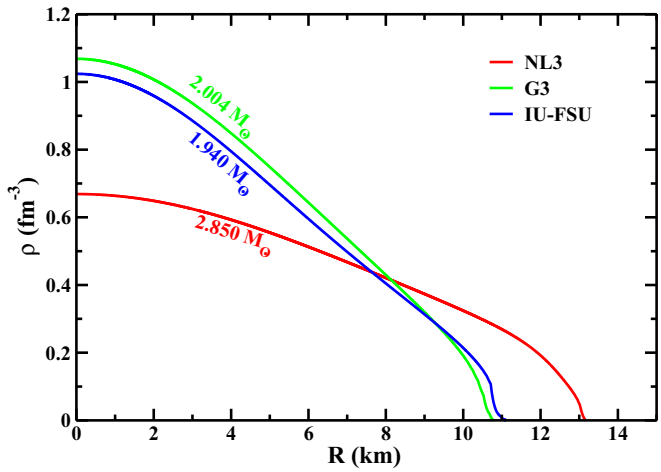

FIG. 3. The neutron star densities (ρ) for NL3 (red), G3 (green), and IU-FSU (blue) parameter sets as a function of radius of the maximum mass star (R). The mass numbers (A) of the maximum mass neutron star for NL3, G3, and IU-FSU are 3.35×10^{54}, 2.32×10^{54}, and 2.23×10^{54} respectively.

and

$$\frac{dP(r)}{dr} = -\frac{[E(r)+P(r)]}{r^2\left(1-\frac{2M(r)}{r}\right)}[M(r)+4\pi r^3 P(r)],$$
$$\frac{dM(r)}{dr} = 4\pi r^2 E(r). \tag{20}$$

Here μ_n, μ_p, μ_e, and μ_μ describe the chemical potentials of the neutrons, protons, electrons, and muons respectively; E and P are the energy density and pressure of the neutron star. The self-consistent numerical solutions of Eqs. (2) and (15) will set the fraction of neutron, proton, electron, and muon number densities for a given baryon density in a neutron star. $M(r)$ is defined as the mass of the neutron star at radius r and the boundary conditions to solve these equations are $P(R) = 0$, for a particular choice of central density $n_c = n(0)$. Finally, we also added the crust part in the above computed EoS to get a detailed and complete analysis of the neutron star properties. We extended the surface part of the NS mathematically by adding the crust energy and pressure calculated by Baym, Pethick, and Sutherland (BPS), in the tail part of all the three RMF parameter's main equation of state [66]. A more detailed formalism to calculate the mass-radius profile of the neutron star using RMF equation of state can be found in Refs. [9,35,41]. The mass-radius profile for all the three assumed parameter sets is shown in Fig. 2.

The maximum masses of the neutron star calculated with the help of G3 and IU-FSU parameter sets are $2.004M_\odot$ and $1.940M_\odot$ respectively [9,70], which fit well in the range of the observational pulsar data PSR J1614-2230 ($M = 1.908 \pm 0.04M_\odot$) [71], PSR J0348 + 0432 ($M = 2.01 \pm 0.04\ M_\odot$) [72], and PSR J0740 + 6620 ($M = 2.15^{+0.10}_{-0.09}M_\odot$) [73]. Recent evaluation of the pulsar data PSR J0740 + 6620 done by Fonseca et al. enumerate the mass of the star in the range $2.08 \pm 0.07M_\odot$ with 68% confidence limit [74]. The old NICER [67,68] data are satisfied by both G3 and IU-FSU sets. Also, recently the new equatorial circumferential radius measurements are reported by Miller *et al.* [69] on the basis of NICER and XMM-Newton x-ray observation of PSR J0740 + 6620 within 68% confidence limit. However, the mass predicted by the NL3 parameter set is quite larger than the defined limit. The radius constraint put recently by the Miller *et al.* using NICER simulations for the canonical star ($1.4M_\odot$) is also well satisfied by the G3 and IU-FSU parameter sets [69]. Also, the constraint set by the observational data of GW170817 event for the tidal deformability of canonical star is satisfied by the G3 parameter set ($\Lambda = 582.26$) [25,35,75]. So, we can claim that the assumed RMF parameter sets are consistent with the astrophysical observational data and well suited to calculate the various properties of neutron star.

The density-radius curve of the neutron star for NL3, G3, and IU-FSU parameter sets is depicted in Fig. 3. The density-radius curve is computed for the maximum mass predicted by the corresponding parameter set, i.e., $2.850M_\odot$ for NL3, $2.004M_\odot$ for G3 and $1.940M_\odot$ for IU-FSU. We observe that the central density of the neutron star is maximum for the G3 parameter set, while NL3 being the stiffest EoS, have the lowest central density.

However, with the help of the density-radius curve, we can calculate the weight function ($|F(x)|^2$) of the neutron star. The total number of nucleons for the neutron star with the maximum mass predicted by NL3, G3, and IU-FSU parameter sets with mass number A are 3.35×10^{54}, 2.32×10^{54}, and 2.23×10^{54} respectively [76]. The total number of nucleons computed for a canonical star are 1.53297×10^{54}, 1.53281×10^{54}, and 1.53286×10^{54} respectively for NL3, G3, and IU-FSU sets. Although the number difference appears after the third decimal for all three forces, actually these numbers are quite different from each other due to the order of magnitude. It is worth mentioning that the neutron star is a big nucleus with nucleons, electrons, and muons, which has variation

TABLE II. The numerical values of incompressibility, symmetric energy, slope, and curvature parameter for maximum mass and the canonical mass star of the corresponding RMF parameter sets. The maximum mass for NL3, G3, and IU-FSU parameter sets are $2.850M_{\odot}$, $2.004M_{\odot}$, and $1.940M_{\odot}$ respectively. All the values are in MeV unit.

	NL3		G3		IU-FSU	
Parameter set	Maximum mass	Canonical mass	Maximum mass	Canonical mass	Maximum mass	Canonical mass
$K^{\rm star}$	44.956	3.934	29.480	3.590	29.827	3.389
$S^{\rm star}$	146.002	15.911	66.813	8.904	60.758	7.228
$L_{\rm sym}^{\rm star}$	615.854	65.038	307.015	45.392	320.321	48.225
$K_{\rm sym}^{\rm star}$	−688.514	−70.534	−360.127	−44.315	−228.012	−26.282

of density with radius as shown in Fig. 3. It possesses all properties of a finite nucleus with mass number A. The giant monopole excitation energy controls by the incompressibility of the nucleus [20,77,78]. Here also $K^{\rm star}$ gives significant information about the giant resonances of the neutron star. With all the input ingredients acquired, we calculate the numerical values of incompressibility, symmetry energy, and its derivatives for maximum mass neutron star and canonical star represented by all the three parameter sets using RMF density functional and CDFM model. Until now, to the best of our knowledge we did not find any work in the literature regarding the availability of exact numerical values of nuclear matter properties of neutron star or any theoretical model which can endue us with such formalism. We here are explicating the numerical values of incompressibility, symmetry energy, slope, and curvature parameter (Table II) of a neutron star for the chosen RMF forces, which is unaccustomed. We deciphered some interesting results from the values of Table II. We observed that the values of all the nuclear properties for maximum mass star with NL3 is greater in comparison to G3 and IU-FSU forces. The magnitude of incompressibility coefficient for maximum mass star with NL3, G3, and IU-FSU parameter sets are 44.956, 29.480, and 29.827 MeV respectively. This tendency of NL3 predicting the higher values of incompressibility and other properties for neutron star justify its nature of stiff EoS, which has also been anticipated for symmetric nuclear matter case [39].

Another important dimension of incompressibility is that the incompressibility of the matter decreases with increase of asymmetricity and density. For example, the incompressibility of pure nuclear matter, i.e., with equal number of protons and neutrons at saturation is 243.96 MeV for G3 set and it is 29.827 MeV for neutron star matter, which has a large asymmetry and density. This decreases in the incompressibility coefficient as we increase the density of the system has also been reported in the literature [9]. The validity of a equation of state can be solely checked by computing its incompressibility coefficient. The numerical range for incompressibility coefficient is indeed the most important quantity to calculate as it restricts the stiffness of the equation of state of the system by checking the compatibility of the equation of state with causality, which require the adiabatic sound speed not to exceed the speed of light [41]. The lowest central density for NL3 parameter set despite being the prediction of highest mass is the result of causality restriction, as the stiffness of the equation of state which is related to the incompressibility should be be compatible with causality at highest density [13]. We realize that the maximally incompressible equation of state can be softed by reducing the K, which in turn will reduce the maximum neutron star mass significantly. To inspect the shift of incompressibility coefficient with the mass of the neutron star, we extend the calculations for different masses using G3 parameter set. We observe that the values of $K^{\rm star}$ with G3, as a representative parameter set, for $1.4M_{\odot}$, $1.6M_{\odot}$, $1.7M_{\odot}$, $1.8M_{\odot}$, and $2.004M_{\odot}$ are 3.590, 5.203, 6.302, 9.163, and 29.480 MeV respectively. However, on the other hand, the incompressibility coefficient of the canonical star is almost same for all the considered RMF parameter sets, given in Table II. This particular observation of the incompressibility coefficient seems to indicate that the value of $K^{\rm star}$ is proportional to the mass of the star, which sequentially depends on the number of nucleons. A more detailed study regarding the observance and conclusions of the correlations between the incompressibility and mass of the neutron star is in progress and will be published elsewhere [79].

The magnitude of the symmetry energy for maximum mass neutron star is also a bit higher in comparison to the magnitude of symmetric nuclear matter at saturation density for all the RMF parameter sets. The numerical values of symmetry energy at saturation density for a symmetric nuclear matter with NL3, G3, and IU-FSU forces are 37.43, 31.84, and 32.71 MeV respectively, while those for the case of maximum mass neutron star comes out to be 146.002, 66.813, and 60.758 MeV. The values of symmetry energy for canonical star is quite smaller in magnitude as compare to maximum mass star of the corresponding RMF parameter set. Also, contrary to the case of incompressibility, in spite of being the same mass of canonical star for all the three parameter sets, the magnitude of the symmetry energy is not equal for different parameter set. This kind of behavior reflects the dependence of symmetry energy on the structure and composition of the neutron star. The incompressibility K is obtained from the derivative of energy density with respect to density, but the symmetry energy is derived from the derivative of the energy density with respect to asymmetry. Thus, it shows a significant variation in the symmetry energy as compared to incompressibility. As we can see from Fig. 2, the radius of canonical star differ for the NL3, G3, and IU-FSU parameters, which cause the change in $S^{\rm star}$ for the same mass of the star.

Although there are no empirical or experimental data available to support the magnitude of the neutron star's symmetry energy, we know that neutron star is a highly asymmetric dense object, so a major change in the symmetry energy with mass is expected due to its isospin-dependent characteristics

and the structural behavior. The unexpectedly larger value of $L_{\rm sym}^{\rm star}$ for NL3 parameter set is also supported by the inclination of stiff EoS of the dense matter toward higher value of slope parameter [21]. A precise knowledge of the range of symmetry energy and $L_{\rm sym}$ is enough to estimate the radius of a neutron star quite perfectly. A well-defined information about the range of symmetry energy and $L_{\rm sym}$ is relevant to trace a more strong and constrained correlation between the surface and volume symmetry energy terms in the mass formula [80]. The static dipole polarizability, quadrupole polarizability, and the neutron skin thickness are closely related to the correlation between symmetry energy and slope parameter [80,81]. Similar to the case of $S^{\rm star}$, the magnitude of slope parameter for canonical star is also significantly smaller in comparison to the maximum mass star for the considered RMF parameter sets. $K_{\rm sym}^{\rm star}$, being the second-order derivative of symmetry energy, is the most sensitive and ambiguous quantity to calculate precisely. The negative magnitude of the curvature parameter corroborated by the 1-σ constraint and 90% confident bounds on its value at saturation density of symmetric nuclear matter, derived by Zimmerman *et al.* using the observational data of PSR J0030 + 0451 and GW170817 event [25,47,68]. Although these bounds are not well suited to discuss the curvature parameter of a neutron star, it implies the possibility of negative magnitude and alludes to the proximity range around the 90% confidence limit of astrophysical observation data. The separation of the contribution of isovector incompressibility or curvature parameter ($K_{\rm sym}$) from the total incompressibility of a matter can be useful for some teresterrial experiments related to exotic nuclei and heavy-ion collisions [82,83]. A more confident theoretical bound on the value of $K_{\rm sym}$ estimated by the present study through RMF parameter sets for neutron star is a better way to tune the experimental techniques related to isoscalar giant resonances toward the prediction of properties related to astrophysical objects. A more detailed study about the importance and correlations of the newly introduced parameters for the neutron star ($X^{\rm star}$) will be published in a future work [79].

Despite the deprivation of direct experimental measurement or empirically acquirable data for the nuclear properties, i.e., incompressibility, symmetry energy, etc., of the neutron star, the numerical values calculated here with the help of consolidated RMF and CDFM formalism appear justifiable. The present theoretical perspective can be validated using various consistent energy density functionals and relevant RMF parameter sets. This accessibility of neutron star properties through a finite nuclei approach favors a stronger correlation between the two unequally sized objects. The theoretical approach employed in this work present new opportunities for nuclear and astrophysicists to unearth information on dense astronautical objects and exotic finite nuclei.

[1] J. M. Lattimer and M. Prakash, Science **304**, 536 (2004).
[2] J. M. Lattimer, Nucl. Phys. A **928**, 276 (2014).
[3] N. Alam, B. K. Agrawal, M. Fortin, H. Pais, C. Providência, A. R. Raduta, and A. Sulaksono, Phys. Rev. C **94**, 052801(R) (2016).
[4] A. S. Schneider, L. F. Roberts, C. D. Ott, and E. O'Connor, Phys. Rev. C **100**, 055802 (2019).
[5] H. Gil, Y.-M. Kim, P. Papakonstantinou, and C. H. Hyun, Phys. Rev. C **103**, 034330 (2021).
[6] Y. Zhang, P. Danielewicz, M. Famiano, Z. Li, W. Lynch, and M. Tsang, Phys. Lett. B **664**, 145 (2008).
[7] K. Hagel, J. B. Natowitz, and G. Röpke, Eur. Phys. J. A **50**, 39 (2014).
[8] R. Wada, K. Hagel, L. Qin, J. B. Natowitz, Y. G. Ma, G. Röpke, S. Shlomo, A. Bonasera, S. Typel, Z. Chen, M. Huang, J. Wang, H. Zheng, S. Kowalski, C. Bottosso, M. Barbui, M. R. D. Rodrigues, K. Schmidt, D. Fabris, M. Lunardon *et al.*, Phys. Rev. C **85**, 064618 (2012).
[9] A. Kumar, H. C. Das, S. K. Biswal, B. Kumar, and S. K. Patra, Eur. Phys. J. C **80**, 775 (2020).
[10] Z. Zhang and L.-W. Chen, Phys. Lett. B **726**, 234 (2013).
[11] L. Trippa, G. Colò, and E. Vigezzi, Phys. Rev. C **77**, 061304(R) (2008).
[12] M. B. Tsang, Y. Zhang, P. Danielewicz, M. Famiano, Z. Li, W. G. Lynch, and A. W. Steiner, Phys. Rev. Lett. **102**, 122701 (2009).
[13] T. S. Olson, Phys. Rev. C **63**, 015802 (2000).
[14] M.-A. Hashimoto, K. Oyamatsu, and Y. Eriguchi, Astrophys. J. **436**, 257 (1994).
[15] G. F. Bertsch, P. F. Bortignon, and R. A. Broglia, Rev. Mod. Phys. **55**, 287 (1983).
[16] F. E. Bertrand, Nucl. Phys. A **354**, 129 (1981).
[17] D. H. Youngblood, Y.-W. Lui, H. L. Clark, B. John, Y. Tokimoto, and X. Chen, Phys. Rev. C **69**, 034315 (2004).
[18] M. Buenerd, J. Phys. Colloques **45**, C4 (1984).
[19] M. Centelles, X. Viñas, S. K. Patra, J. N. De, and T. Sil, Phys. Rev. C **72**, 014304 (2005).
[20] S. Patra, X. Viñas, M. Centelles, and M. Del Estal, Nucl. Phys. A **703**, 240 (2002).
[21] I. Bednarek, J. Sadkowski, and J. Syska, Symmetry **12**, 898 (2020).
[22] J. M. Lattimer, Annu. Rev. Nucl. Part. Sci. **62**, 485 (2012).
[23] L. Engvik, M. Hjorth-Jensen, E. Osnes, G. Bao, and E. Østgaard, Phys. Rev. Lett. **73**, 2650 (1994).
[24] I. Bombaci and D. Logoteta, Astron. Astrophys. **609**, A128 (2018).
[25] B. P. Abbott *et al.* (LIGO Scientific Collaboration and Virgo Collaboration), Phys. Rev. Lett. **119**, 161101 (2017).
[26] J. Boguta, Phys. Lett. B **106**, 255 (1981).
[27] C. X.-R. Observatory, https://www.nasa.gov/mission_pages/chandra/main/index.html.
[28] S. K. Greif, K. Hebeler, J. M. Lattimer, C. J. Pethick, and A. Schwenk, Astrophys. J. **901**, 155 (2020).
[29] T. H. R. Skyrme and B. F. J. Schonland, Proc. R. Soc. London, Ser. A **260**, 127 (1961).
[30] J. Dechargé and D. Gogny, Phys. Rev. C **21**, 1568 (1980).
[31] J. Walecka, Ann. Phys. **83**, 491 (1974).
[32] Y. Gambhir, P. Ring, and A. Thimet, Ann. Phys. **198**, 132 (1990).
[33] C. Adam, A. G. Martn-Caro, M. Huidobro, R. Vzquez, and A. Wereszczynski, Phys. Lett. B **811**, 135928 (2020).

[34] C. Adam, M. Haberichter, and A. Wereszczynski, Phys. Rev. C **92**, 055807 (2015).
[35] B. Kumar, S. K. Patra, and B. K. Agrawal, Phys. Rev. C **97**, 045806 (2018).
[36] B. Kumar, S. Singh, B. Agrawal, and S. Patra, Nucl. Phys. A **966**, 197 (2017).
[37] S. S. Avancini, M. E. Bracco, M. Chiapparini, and D. P. Menezes, Phys. Rev. C **67**, 024301 (2003).
[38] S. K. Singh, S. K. Biswal, M. Bhuyan, and S. K. Patra, Phys. Rev. C **89**, 044001 (2014).
[39] G. A. Lalazissis, J. König, and P. Ring, Phys. Rev. C **55**, 540 (1997).
[40] A. Carbone and A. Schwenk, Phys. Rev. C **100**, 025805 (2019).
[41] H. C. Das, A. Kumar, B. Kumar, S. K. Biswal, T. Nakatsukasa, A. Li, and S. K. Patra, Mon. Not. R. Astron. Soc. **495**, 4893 (2020).
[42] U. Garg and G. Col, Prog. Part. Nucl. Phys. **101**, 55 (2018).
[43] P. Danielewicz and J. Lee, Nucl. Phys. A **922**, 1 (2014).
[44] H. C. Das, A. Kumar, and S. K. Patra, Phys. Rev. D **104**, 063028 (2021).
[45] P. Zyla, R. Barnett, J. Beringer *et al.*, Prog. Theoretical Experimental Physics **2020**, 063028 (2020).
[46] H. A. Bethe, Annu. Rev. Nucl. Sci. **21**, 93 (1971).
[47] J. Zimmerman, Z. Carson, K. Schumacher, A. W. Steiner, and K. Yagi, arXiv:2002.03210 [astro-ph.HE].
[48] K. A. Brueckner, S. A. Coon, and J. Dabrowski, Phys. Rev. **168**, 1184 (1968).
[49] K. A. Brueckner, J. R. Buchler, S. Jorna, and R. J. Lombard, Phys. Rev. **171**, 1188 (1968).
[50] F. Coester, B. Day, and A. Goodman, Phys. Rev. C **5**, 1135 (1972).
[51] A. Kumar, H. C. Das, M. Kaur, M. Bhuyan, and S. K. Patra, Phys. Rev. C **103**, 024305 (2021).
[52] A. Antonov, V. Nikolaev, and I. Petkov, Zeitschr. Phys. A **297**, 257 (1980).
[53] A. N. Antonov, D. N. Kadrev, and P. E. Hodgson, Phys. Rev. C **50**, 164 (1994).
[54] M. Gaidarov, I. Moumene, A. N. Antonov, D. N. Kadrev, P. Sarriguren, and E. M. Guerra, Nucl. Phys. A **1004**, 122061 (2020).
[55] M. K. Gaidarov, A. N. Antonov, P. Sarriguren, and E. Moya de Guerra, Phys. Rev. C **84**, 034316 (2011).
[56] M. Kaur, A. Quddus, A. Kumar, M. Bhuyan, and S. Patra, J. Phys. G **47**, 105102 (2020).
[57] A. N. Antonov, D. N. Kadrev, M. K. Gaidarov, P. Sarriguren, and E. Moya de Guerra, Phys. Rev. C **98**, 054315 (2018).
[58] A. N. Antonov, M. K. Gaidarov, P. Sarriguren, and E. Moya de Guerra, Phys. Rev. C **94**, 014319 (2016).
[59] M. K. Gaidarov, A. N. Antonov, P. Sarriguren, and E. Moya de Guerra, Phys. Rev. C **85**, 064319 (2012).
[60] A. L. Fetter and J. D. Walecka, *Quantum Theory of Many-Particle Systems* (McGraw-Hill, Boston, 1971).
[61] L.-W. Chen, B.-J. Cai, C. M. Ko, B.-A. Li, C. Shen, and J. Xu, Phys. Rev. C **80**, 014322 (2009).
[62] W.-C. Chen and J. Piekarewicz, Phys. Rev. C **90**, 044305 (2014).
[63] F. Pacini, memsai **36**, 323 (1965).
[64] J. R. Oppenheimer and G. M. Volkoff, Phys. Rev. **55**, 374 (1939).
[65] R. C. Tolman, Phys. Rev. **55**, 364 (1939).
[66] G. Baym, C. Pethick, and P. Sutherland, Astrophys. J. **170**, 299 (1971).
[67] M. C. Miller, F. K. Lamb, A. J. Dittmann *et al.*, Astrophys. J. **887**, L24 (2019).
[68] T. E. Riley, A. L. Watts, S. Bogdanov, P. S. Ray, R. M. Ludlam, S. Guillot, Z. Arzoumanian, C. L. Baker, A. V. Bilous, D. Chakrabarty, K. C. Gendreau, A. K. Harding, W. C. G. Ho, J. M. Lattimer, S. M. Morsink, and T. E. Strohmayer, Astrophys. J. **887**, L21 (2019).
[69] M. C. Miller, F. K. Lamb, A. J. Dittmann, S. Bogdanov, Z. Arzoumanian, K. C. Gendreau, S. Guillot, W. C. G. Ho, J. M. Lattimer, M. Loewenstein, S. M. Morsink, P. S. Ray, M. T. Wolff, C. L. Baker, T. Cazeau, S. Manthripragada, C. B. Markwardt, T. Okajima, S. Pollard, I. Cognard *et al.*, Astrophys. J. Lett. **918**, L28 (2021).
[70] H. C. Das, A. Kumar, B. Kumar, S. K. Biswal, and S. K. Patra, J. Cosmol. Astropart. Phys. **2021**, 007 (2021).
[71] Z. Arzoumanian, A. Brazier, S. Burke-Spolaor, S. Chamberlin, S. Chatterjee, B. Christy, J. M. Cordes, N. J. Cornish, F. Crawford, H. T. Cromartie, K. Crowter, M. E. DeCesar, P. B. Demorest, T. Dolch, J. A. Ellis, R. D. Ferdman, E. C. Ferrara, E. Fonseca, N. Garver-Daniels, P. A. Gentile *et al.*, Astrophys. J. Suppl. Ser. **235**, 37 (2018).
[72] J. Antoniadis, P. C. C. Freire, N. Wex, T. M. Tauris, R. S. Lynch, M. H. van Kerkwijk, M. Kramer, C. Bassa, V. S. Dhillon, T. Driebe, J. W. T. Hessels, V. M. Kaspi, V. I. Kondratiev, N. Langer, T. R. Marsh, M. A. McLaughlin, T. T. Pennucci, S. M. Ransom, I. H. Stairs, J. van Leeuwen *et al.*, Science **340**, 1233232 (2013).
[73] H. T. Cromartie, E. Fonseca, S. M. Ransom, P. B. Demorest, Z. Arzoumanian, H. Blumer, P. R. Brook, M. E. DeCesar, T. Dolch, J. A. Ellis *et al.*, Nature Astron. **4**, 72 (2019).
[74] E. Fonseca, H. T. Cromartie, T. T. Pennucci, P. S. Ray, A. Y. Kirichenko, S. M. Ransom, P. B. Demorest, I. H. Stairs, Z. Arzoumanian, L. Guillemot *et al.*, Astrophys. J. Lett. **915**, L12 (2021).
[75] H. C. Das, A. Kumar, and S. K. Patra, Monthly Notices Royal Astron. Soc. **507**, 4053 (2021).
[76] N. K. Glendenning, *Compact Stars: Nuclear Physics, Particle Physics, and General Relativity* (Springer, New York, 1997).
[77] S. K. Patra, B. K. Raj, M. S. Mehta, and R. K. Gupta, Phys. Rev. C **65**, 054323 (2002).
[78] S. Patra, M. Centelles, X. Viñas, and M. Del Estal, Phys. Lett. B **523**, 67 (2001).
[79] J. A. Pattnaik, A. Kumar, H. C. Das, M. Bhuyan, and S. K. Patra (unpublished).
[80] J. M. Lattimer, in *Exotic Nuclei and Nuclear/Particle Astrophysics (V) From Nuclei to Stars: Carpathian Summer School of Physics 2014*, American Institute of Physics Conference Series Vol. 1645 (AIP, New York, 2015), pp. 61–78.
[81] J. M. Lattimer and Y. Lim, Astrophys. J. **771**, 51 (2013).
[82] L.-W. Chen, C. M. Ko, and B.-A. Li, Phys. Rev. C **76**, 054316 (2007).
[83] M. Centelles, X. Roca-Maza, X. Viñas, and M. Warda, Phys. Rev. Lett. **102**, 122502 (2009).